Proceedings of the 9th World Congress on Mechanical, Chemical, and Material Engineering (MCM'23)
Brunel University, London, United Kingdom –August 06-08, 2023
Paper No. HTFF 173
DOI: 10.11159/htff23.173

Molecular Dynamics Simulation of Adiabatic Two-Phase Flow in Nanochannels

Yunmin Ran[1], Volfango Bertola[1]
[1] Laboratory of Technical Physics, School of Engineering, University of Liverpool, Brownlow Hill, Liverpool L69 3GH, United Kingdom
Yunmin.Ran@liverpool.ac.uk; Volfango.Bertola@liverpool.ac.uk

Abstract **-** The two-phase flow of argon fluid in a nanochannel is investigated by molecular dynamics simulations (MDS). The nanochannel consists of two parallel copper plates with the length of 2000 Å and the height of 120 Å, where the density of liquid argon is 1316.5 kg/m^3 at 100 K. An external driving force, ranging from 0.001 to 0.005 eV/ Å, was applied along the flow direction to fluid particles at the channel inlet during simulations. The flow patterns were obtained from the density distribution. Based on flow patterns, the void fraction was discussed as a function of the mean flow velocity. When the initial filling ratio is 67 %, the void fractions of different velocities are all close to 33%, which means these simulations are consistent with the homogeneous model. Different filling ratios were also analysed. As the filling ratio is increased, the bubble size decreases and the void fraction also decreases. Molecular dynamics simulation show that under these conditions the flow is adequately described by the homogeneous model.

Keywords**:** Two-phase flow, Molecular dynamics simulation, Nanochannels, Void fraction.

1. Introduction

Microfabrication or nanotechnology originated as techniques developed for integrated circuits, and has rapidly expanded into areas such as bioengineering and biotechnology, aerospace, micro heat exchangers, microelectronics, materials processing, and thin film deposition. Due to the cooling requirements of electronic components and devices, micro- and nanoscale heat transfer technologies such as micro heat exchangers with nanochannels have been developed. Compared with single-phase heat transfer in a nanochannel, the small cross-sectional area along with with phase change can produce very high heat transfer coefficients with relatively small flow rates, and provide better heat transfer performance [1-4].

There is no doubt that the flow patterns in micro- or nanochannels are different from those in macro channels [5]. Many experiments were conducted to characterise the flow patterns in microchannels with circular and rectangular cross-sections [6-10]. Triplett et. al [6, 7] conducted air-water two-phase flow experiments in 1.1 mm and 1.45 mm i.d. circular channels as well as in channels with semi-triangular cross-section having 1.09 mm and 1.49 mm hydraulic diameters. They observed five different flow patterns: bubbly, slug, churn, slug-annular and annular flow, respectively. The void fraction and pressure drop were best predicted by the homogeneous model assumption. Chung and Kawaji [8] investigated the flow patterns of a mixture of nitrogen gas and water in circular channels of 530, 250, 100, and 50 μm diameter. Based on the flow regime map, void fraction, and frictional pressure drop, they found that in the 530 and 250 μm channels the two-phase flow characteristics were similar to those typically observed in mini-channels. However, in the 100 and 50 μm channels the void faction-volumetric quality relationship departs from the typical linear correlation proposed by Armand [11]. Choi et. al [10] studied the effect of the aspect ratio on the flow pattern, pressure drop and void fraction with liquid water and nitrogen gas two-phase flow in rectangular microchannels. They found that there is a linear relation between the void fraction and volumetric quality and the two-phase flow becomes homogenous with decreasing the aspect ratio.

Generally, the void fraction is expressed as a function of the volumetric quality (i.e., the gas fraction of volume flow). Armand [11] proposed a linear void fraction correlation, which is verified by various experiments [5, 12, 13] for volumetric qualities up to ~80%. However, when the hydraulic diameter is smaller than 100 μm, non-linear correlations are more accurate [8, 9, 14]. When the channel size is decreased further in the micro- or nanoscale, the experimental difficulty in measuring the void fraction increases, resulting into poorer accuracy. Thus, numerical simulations can provide easier access to quantities that are not accessible experimentally. Fukagata et. al [15] carried out numerical simulations of air-water two-

phase flows in 20 μm micro-tubes. They found the void fraction is in good agreement with the correlations proposed for macroscopic flows, but the frictional pressure drop was found to be higher than the experimental results. They also observed the length of the computational domain considerably affects the flow pattern resulting from simulations. Mukherjee and Kandlikar [16] numerically investigated the fluid flow and heat transfer features associated with slug flow boiling in a square microchannel. The VOF method was adopted to capture the interface dynamics. Compared with circular channels, the velocity of the bubble in a square channel is always larger, and the bubble interface at the corners and faces of the square cross-section induce transversal flows, which decreases the liquid film thickness of the bubble. Magnini et. al [17] carried out flow boiling simulations with three different refrigerant fluids in a circular channel of 0.5 mm diameter. They found the high liquid-to-vapor density ratio leads to a rapidly expanding bubble and the heat transfer coefficient increases monotonically as the film thickness decreases. Thin-film evaporation was proven to be the dominant heat transfer mechanism in the liquid film region between the wall and the elongated bubble, while transient heat convection was found to strongly enhance the heat transfer performance in the bubble wake in the liquid slug between two bubbles. Zhang and Jia [18] carried out a three-dimensional numerical investigation of flow boiling based on the interfacial temperature gradient model. They observed the transition of flow patterns from bubbly flow to slug flow and annual flow. Results showed that the local heat transfer coefficients are significantly influenced by the flow patterns.

Compared with the traditional numerical analysis methods, molecular dynamics simulation (MDS) presents the trajectories of single atoms and molecules as a function of time. MDS is applied to analyse the physical movements of atoms and molecules, which are allowed to interact for a fixed period of time. Since it relies on the numerical solution of Newton's equations of motion for a system of interacting particles, MDS can give clear patterns of the heat transfer process from atoms and molecules when the system is in micro- and nanoscale. In the present work, molecular dynamics simulations are used to investigate the two-phase flow patterns and void fraction in nanochannels. Results are compared with previous numerical and experimental data, and provide a starting point for the development of molecular simulations of multiphase flows.

2. Method

Molecular dynamics simulations were carried out with the open-source software LAMMPS (Large-scale Atomic/Molecular Massively Parallel Simulator) [19]. The three-dimensional molecular system consisted of two solid copper infinite parallel walls, containing argon fluid. The thickness of each wall was 8 Å and the fluid domain was a channel with the height of H=120 Å and length of L=2000 Å. A lattice structure of face-centred cubic (FCC) unit cells with lattice constant a=3.61 Å was used to model the solid walls. Initially, the fluid region was partially filled with liquid at equilibrium with its vapour. With different filling ratios, the argon atoms were distributed between the two walls according to the densities of the liquid and vapour phases in each zone. The wall and fluid temperature were initially set at 100 K, and the density of liquid argon was 1316.5 kg/m^3. The interatomic interactions between the argon atoms as well as those between the copper and the argon atoms were described by the Lennard-Jones (LJ) 12-6 model potential, which is written as:

$$\varphi(r_{ij}) = 4\alpha\left[\left(\frac{\sigma}{r_{ij}}\right)^{12} - \left(\frac{\sigma}{r_{ij}}\right)^{6}\right] \tag{1}$$

where the α is the energy parameter, σ is the length parameter, r_{ij} is the distance between atoms, and the subscripts i and j represent the atoms i and j, respectively. For the fluid-fluid interaction, the LJ potential was applied to argon atoms with length parameter σ_1=0.341 nm and energy parameter α_1=0.0104 eV. The LJ potential was also applied to argon and copper atoms, according to the Lorentz-Berthelot mixing rule:

$$\alpha_{Ar-Cu} = \sqrt{\alpha_{Ar-Ar} \times \alpha_{Cu-Cu}} \tag{2}$$

$$\sigma_{Ar-Cu} = \frac{\sigma_{Ar-Ar} + \sigma_{Cu-Cu}}{2} \tag{3}$$

The embedded atoms method (EAM) potential was used to define interactions between copper atoms.

$$U = \sum_i F_i\left(\sum_{j\neq i} f_i(r_{ij})\right) + \frac{1}{2}\sum_{j\neq i} \varphi_{ij}(r_{ij}) \tag{4}$$

where F_i is the embedding energy, which is a function of the atomic electron density, ρ_i, and α is a pair potential interaction.

In the classical MD method, Newton's equations of motion are solved for atoms and molecules, i.e.:

$$\vec{F_i}(t) = m_i\vec{a_i} = m_i\frac{d^2\vec{r_i}}{dt^2} \tag{5}$$

where t denotes time, and $\vec{F_i}$, m_i, $\vec{r_i}$ are the force vector, mass, and the position vector of molecule i, respectively.

A periodic boundary condition was applied in X and Y directions, which means particles could exit one end of the box and re-enter the other end so that they could interact across the boundary. In the Z direction, the system was bounded by two solid walls. An external driving force in the X direction was applied on the argon molecules before the channel inlet in order to generate the flow. However, this artificially increases the inlet temperature, therefore it was necessary to reset the inlet temperature using the temperature control strategy schematically illustrated in Fig.1. In particular, the fluid domain was divided into five zones: D1 is the forcing zone (-88 Å < x < -84 Å), where an external force f_x is applied to each argon atom; D2 is the buffer zone (-84 Å < x < -44 Å), which allows relaxation between the forcing zone and temperature reset zone and prevents the atoms in these two regions from interacting with one another; D3 is the temperature reset zone (-44 Å < x < -40 Å), the fluid temperature is reset by explicitly rescaling the fluctuating velocity components. Finally, D4 is an additional relaxation zone (-40 Å < x < 0 Å) before the channel, D5.

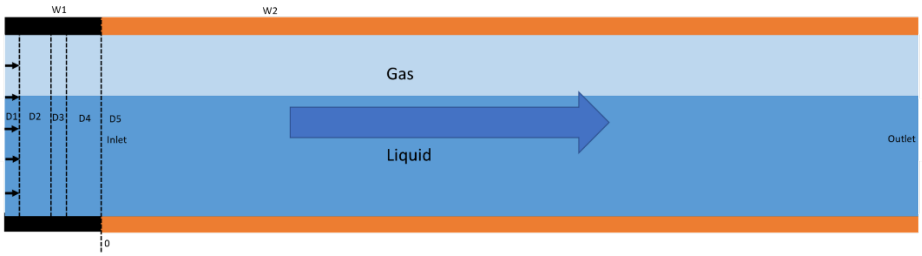

Fig. 1: Schematic of the simulation domain. D1: the forcing zone; D2: the buffer zone; D3: the temperature reset zone; D4: the relaxation zone; D5: the data collection zone.

A series of preliminary simulations showed that when the channel walls are heated or cooled to simulate heat transfer problems, although the fluid temperature is reset in zone D3, atoms in D3 are inevitably affected by the temperature gradients existing between the walls and the fluid, therefore it is necessary to add an additional relaxation zone, D4, to mitigate this interference.

A timestep of Δt =1.0 fs was used in all simulations. Simulations were conducted in three steps. First, the whole system was relaxed in the NVT ensemble (Nose-Hoover thermostat) to 100 K for 0.1 ns. Then, the NVE ensemble was applied to the walls and argon atoms for the next 5.0 ns to make the flow fully developed; the Langevin thermostat was applied to walls in order to maintain their temperature exactly at 100 K. The external force was added to each argon atom in zone D1 of the simulation domain. In the temperature reset zone, the velocity of each atom was reset after removing the streaming velocity of each sub-zone. The streaming velocity was then added back to the flow in the following zone. After the flow was fully developed, the simulation was run for further 5.0 ns to collect fluid flow data. In this study, different velocities and filling ratios of argon fluid are discussed. To obtain the flow patterns and the density distributions, the fluid region was divided into several bins with size 4 × 60 × 4 Å^3.

3. Results and discussion

Fig. 2 shows the density distribution of the fluid with initial filling ratio r = 67%. From the figure, one can observe the formation of an elongated bubble moving between the channel walls.

For the sake of simplicity, the density was reduced to a dimensionless form, and displayed as a binary contour plot as shown in Fig. 3, which presents the flow patterns observed when the streaming velocity (i.e., the force applied to each molecule in zone D1 of the simulation domain) is increased, at constant filling ratio r = 67%. In all cases, the flow pattern consists of a single elongated bubble. In addition, the shape and size of the bubbles are not affected by the mean flow velocity.

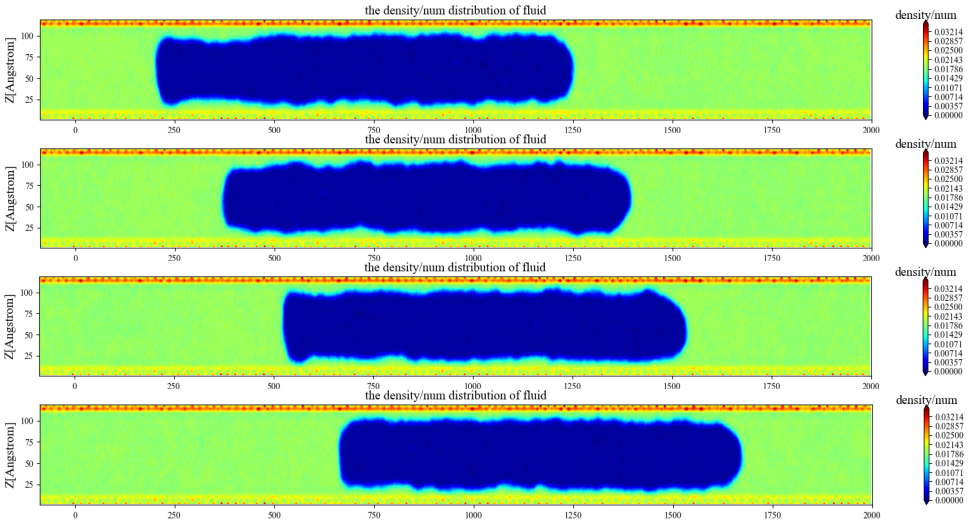

Fig. 2: Snapshots of fluid density distribution at different times, with a filling ratio of 67 % (time = 0.1, 0.2, 0.3, 0.4 ns).

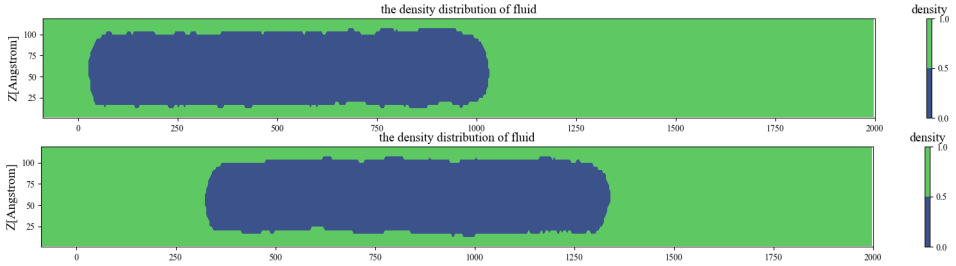

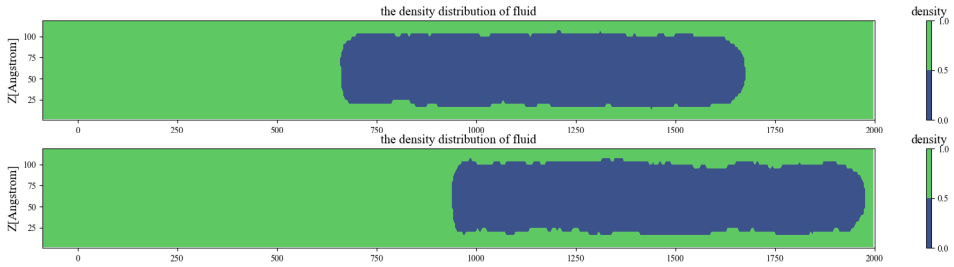

Fig. 3: Snapshots of fluid density distribution with different external force, filling ratio=67 % (f_x=0.0015,0.0020,0.0025,0.0030 eV/ Å).

One of the most significant parameters used to characterize two-phase flows is the void fraction, ε, which is defined as the ratio of the volume of the gaseous phase occupied in a channel to the total volume of the channel at a certain instant of time:

$$\varepsilon = \frac{V_g}{V_g + V_l} \tag{6}$$

where V_g is the volume of the channel occupied by the vapor phase and V_l is that of the liquid phase. If the two phases travel at the same velocity, the flow is called homogeneous, and the void fraction is equal to the gas fraction of volume flow, ε^*, which in the present work is set by the filling ratio:

$$\varepsilon^* = 1 - r \tag{7}$$

Fig. 4 shows the void fraction as a function of the mean flow velocity (which is determined by the external force applied to molecules) at r = 67%. The discontinuous line represents the gas fraction of volume flow. One can observe the void fraction remainss constant and is independent the flow velocity. Thus, the void fraction data indicate the simulation is consistent with the homogenous model.

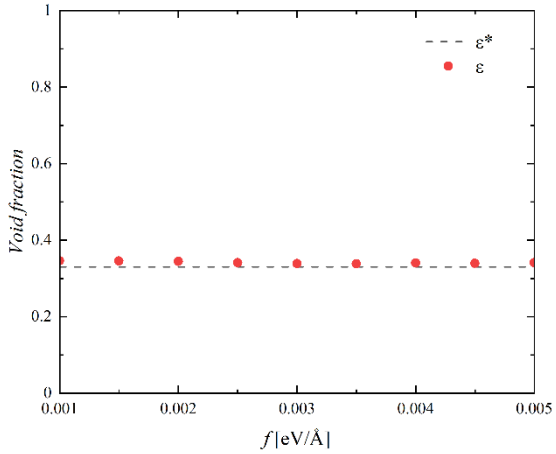

Fig. 4: Void fractions of fluid with different streaming velocities at r=67%.

Fig. 5 shows the density distribution with different filling ratios. Aas the filling ratio increased, the bubble size decreased.

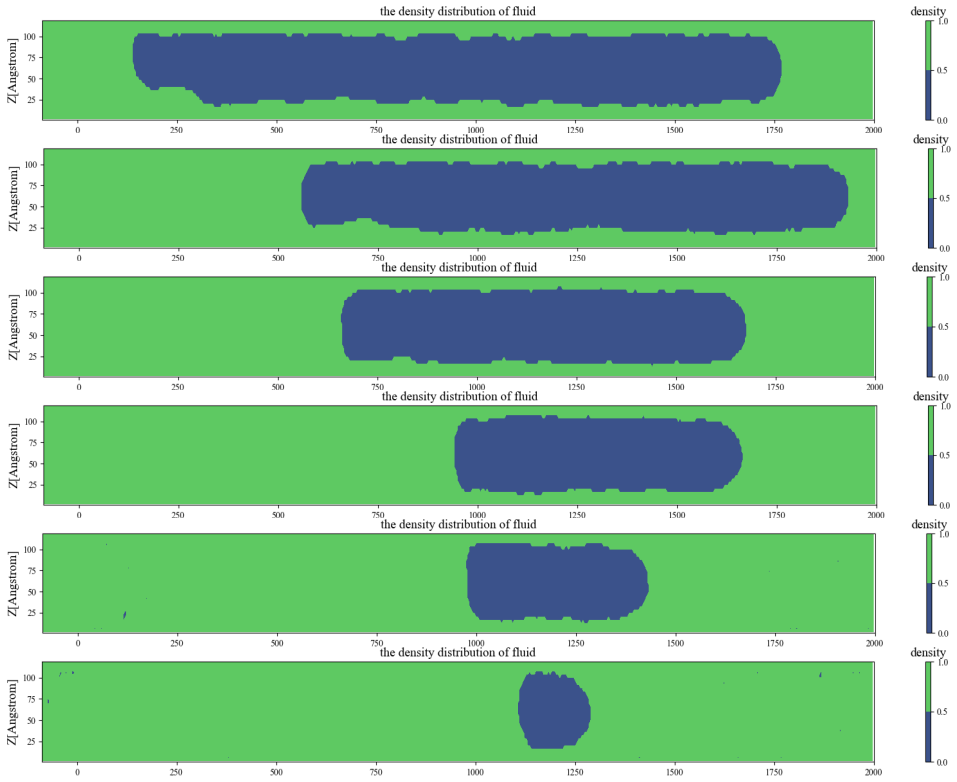

Fig. 5: The flow patterns of fluid with different filling ratios, r=50%,58%,67%,75%,83%,92%

Fig.6 is the void fraction with different filling ratios. With the filling ratio increasing, the void fraction decreased. This result also demonstrates that this molecular dynamics simulation is consistent with the homogeneous model.

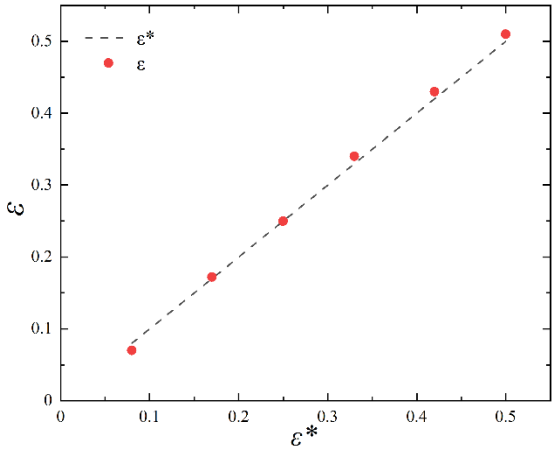

Fig. 6: Void fractions of fluid with different filling ratios.

4. Conclusion

The molecular dynamics simulation of the two-phase flow of argon fluid at 100 K between two parallel copper plates plates with the length of 2000 Å and the height of 120 Å was carried out using the LAMMPS solver. Flow patterns were obtained from the density distributions. Based on flow patterns, the void fractions obtained at different flow rates were discussed. When the filling ratio was set at 67%, the void fractions of different velocities were all quite close to 33%, which which means these simulations are consistent with the homogeneous model. On the other hand, different filling ratios were also analysed, both flow patterns and void fractions. With the increase of the filling ratio, the bubble size decreased and the void fraction also decreased. All simulations consistently indicate that, in the range of the simulation parameters considered, the liquid-vapour flow remains homogeneous.

Acknowledgements

Y. R. gratefully acknowledges financial support from the China Scholarship Fund (CSC). Supercomputing time on ARCHER is provided by the "UK Consortium on Mesoscale Engineering Sciences (UKCOMES)" under the UK Engineering and Physical Sciences Research Council Grants No. EP/R029598/1 and EP/X035875/1. This work made use of computational support by CoSeC, the Computational Science Centre for Research Communities, through UKCOMES. For the purpose of open access, the authors have applied a Creative Commons Attribution (CC-BY) licence to any Author Accepted Manuscript version arising from this submission.

References

[1] X. Peng and B.-X. Wang, "Forced convection and flow boiling heat transfer for liquid flowing through microchannels," *Int J Heat Mass Tran,* vol. 36, no. 14, pp. 3421-3427, 1993.

[2] M. Bowers and I. Mudawar, "High flux boiling in low flow rate, low pressure drop mini-channel and micro-channel heat sinks," *Int J Heat Mass Tran,* vol. 37, no. 2, pp. 321-332, 1994.

[3] M. B. Bowers and I. Mudawar, "Two-phase electronic cooling using mini-channel and micro-channel heat sinks: part 1—design criteria and heat diffusion constraints," 1994.

[4] M. B. Bowers and I. Mudawar, "Two-phase electronic cooling using mini-channel and micro-channel heat sinks: Part 2—Flow rate and pressure drop constraints," 1994.

[5] A. Serizawa, Z. Feng, and Z. Kawara, "Two-phase flow in microchannels," *Experimental Thermal and Fluid Science,* vol. 26, no. 6-7, pp. 703-714, 2002.

[6] K. A. Triplett, S. Ghiaasiaan, S. Abdel-Khalik, and D. Sadowski, "Gas–liquid two-phase flow in microchannels Part I: two-phase flow patterns," *International Journal of Multiphase Flow,* vol. 25, no. 3, pp. 377-394, 1999.

[7] K. Triplett, S. Ghiaasiaan, S. Abdel-Khalik, A. LeMouel, and B. McCord, "Gas–liquid two-phase flow in microchannels: part II: void fraction and pressure drop," *International Journal of Multiphase Flow,* vol. 25, no. 3, pp. 395-410, 1999.

[8] P.-Y. Chung and M. Kawaji, "The effect of channel diameter on adiabatic two-phase flow characteristics in microchannels," *International journal of multiphase flow,* vol. 30, no. 7-8, pp. 735-761, 2004.

[9] R. Xiong and J. Chung, "An experimental study of the size effect on adiabatic gas-liquid two-phase flow patterns and void fraction in microchannels," *Physics of Fluids,* vol. 19, no. 3, p. 033301, 2007.

[10] C. Choi, D. Yu, and M. Kim, "Adiabatic two-phase flow in rectangular microchannels with different aspect ratios: Part I–Flow pattern, pressure drop and void fraction," *Int J Heat Mass Tran,* vol. 54, no. 1-3, pp. 616-624, 2011.

[11] A. A. Armand, "The resistance during the movement of a two-phase system in horizontal pipes," *Izv. Vses. Teplotekh. Inst.,* vol. 15, pp. 16-23, 1946.
[12] A. Kawahara, M. Sadatomi, K. Nei, and H. Matsuo, "Experimental study on bubble velocity, void fraction and pressure drop for gas–liquid two-phase flow in a circular microchannel," *International Journal of Heat and Fluid Flow,* vol. 30, no. 5, pp. 831-841, 2009.
[13] V. Haverkamp, V. Hessel, H. Löwe, G. Menges, M. J. F. Warnier, E. V. Rebrov, M. H. J. M. de Croon, J. C. Schouten, M. A. Liauw, "Hydrodynamics and mixer-induced bubble formation in micro bubble columns with single and multiple-channels," *Chemical Engineering & Technology: Industrial Chemistry-Plant Equipment-Process Engineering-Biotechnology,* vol. 29, no. 9, pp. 1015-1026, 2006.
[14] A. Kawahara, P.-Y. Chung, and M. Kawaji, "Investigation of two-phase flow pattern, void fraction and pressure drop in a microchannel," *International journal of multiphase flow,* vol. 28, no. 9, pp. 1411-1435, 2002.
[15] K. Fukagata, N. Kasagi, P. Ua-arayaporn, and T. Himeno, "Numerical simulation of gas–liquid two-phase flow and convective heat transfer in a micro tube," *International Journal of Heat and Fluid Flow,* vol. 28, no. 1, pp. 72-82, 2007.
[16] A. Mukherjee and S. Kandlikar, "The effect of inlet constriction on bubble growth during flow boiling in microchannels," *Int J Heat Mass Tran,* vol. 52, no. 21-22, pp. 5204-5212, 2009.
[17] M. Magnini, B. Pulvirenti, and J. R. Thome, "Numerical investigation of hydrodynamics and heat transfer of elongated bubbles during flow boiling in a microchannel," *Int J Heat Mass Tran,* vol. 59, pp. 451-471, 2013.
[18] P. Zhang and H. Jia, "Evolution of flow patterns and the associated heat and mass transfer characteristics during flow boiling in mini-/micro-channels," *Chemical Engineering Journal,* vol. 306, pp. 978-991, 2016.
[19] S. Plimpton, "Fast Parallel Algorithms for Short-Range Molecular-Dynamics," (in English), *J Comput Phys,* vol. 117, no. 1, pp. 1-19, Mar 1 1995, doi: DOI 10.1006/jcph.1995.1039.